Electronic Supplementary Material (ESI) for RSC Applied Polymers.
This journal is © The Royal Society of Chemistry 2024

ELECTRONIC SUPPLEMENTARY INFORMATION

Role of polymer interactions in core-shell filaments on mechanical properties of 3D printed objects

Jia-Ruey Ai,[1] Seokhoon Jang,[1] Wyatt Fink,[2] Seong H. Kim,[1] Bryan D. Vogt[1,*]

[1]Department of Chemical Engineering, The Pennsylvania State University, University Park, PA 16802
[2]Department of Engineering Science, The Pennsylvania State University, University Park, PA 16802

*To whom correspondence should be addressed: bdv5051@psu.edu

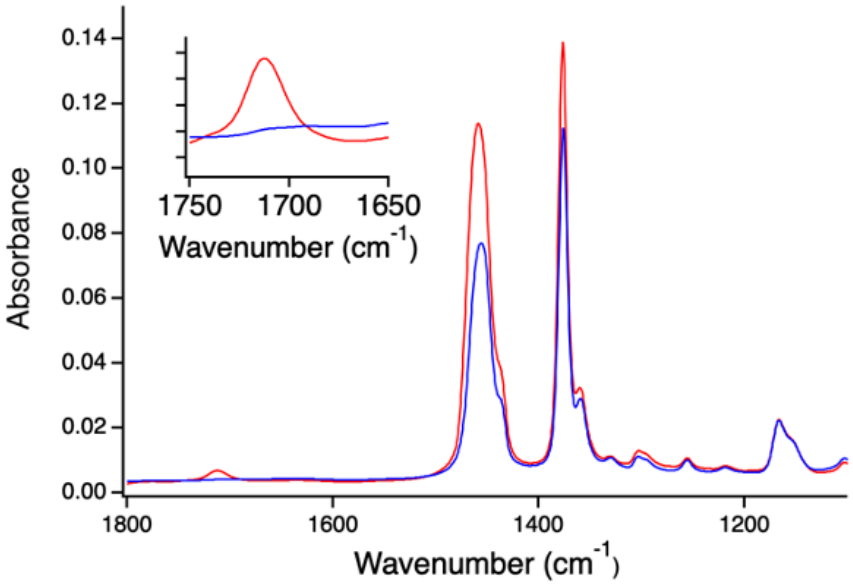

Figure S1. FTIR spectra of as received iPP (blue) and miPP (red). The peak at 1713 cm^{-1} is associated with the carboxylic dimer acid from hydrolysis of the maleic anhydride. Heating converts the acid to the anhydride.

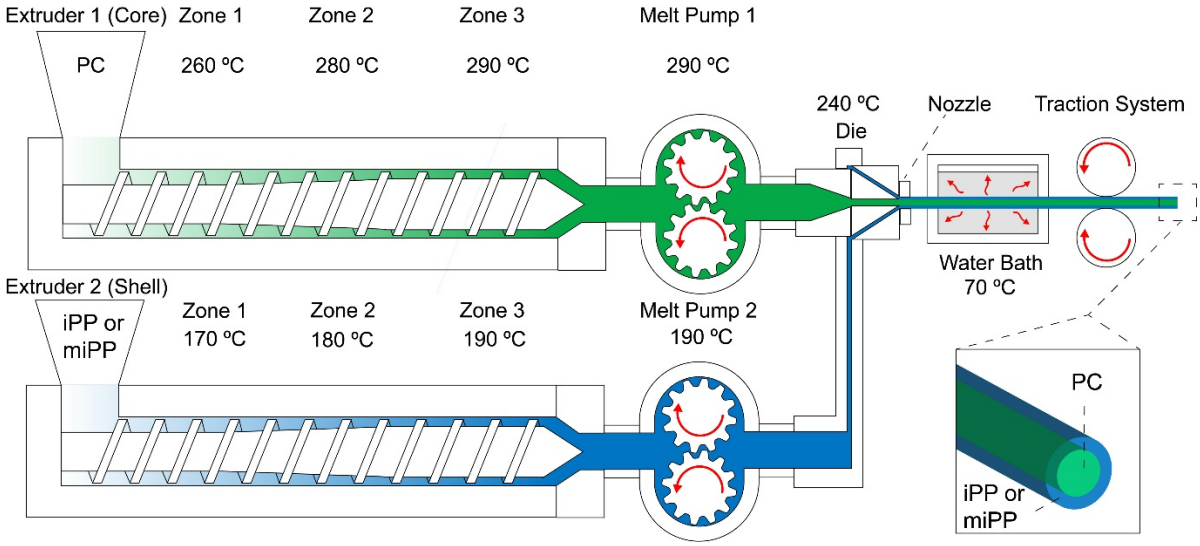

Figure S2. Set up of co-extrusion line for fabricating core-shell structured filament. Alone with processing temperature. While producing single component filament, the extruder 2 is detached. The die used is switched to a 2.2 mm circular die for the single component.

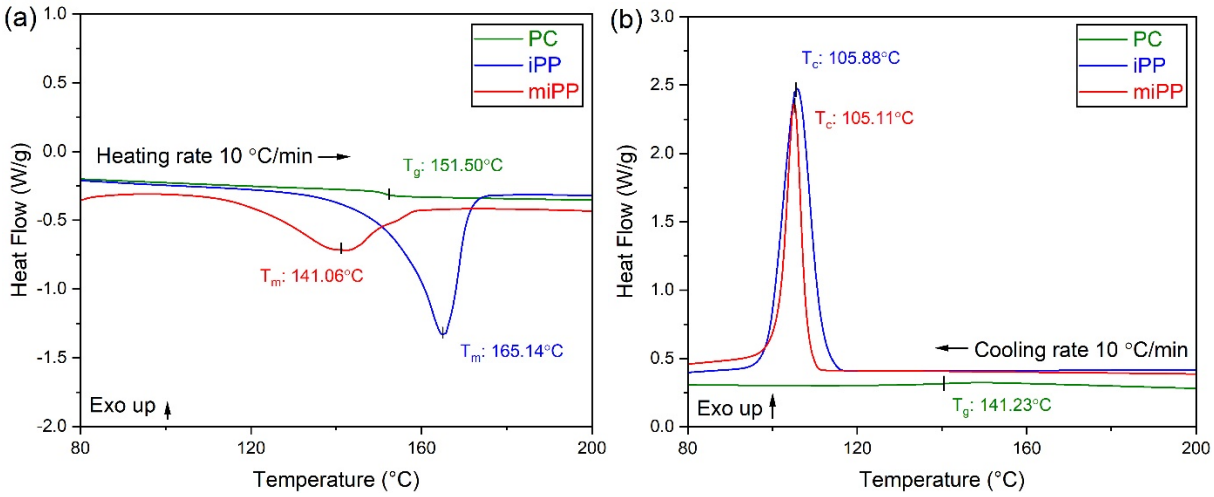

Figure S3. DSC thermograms for (a) first heating and (b) cooling curve for iPP, mPP, and PC. The maleation does not significantly impact the crystallization, but the melting point is suppressed due to smaller average crystal size.

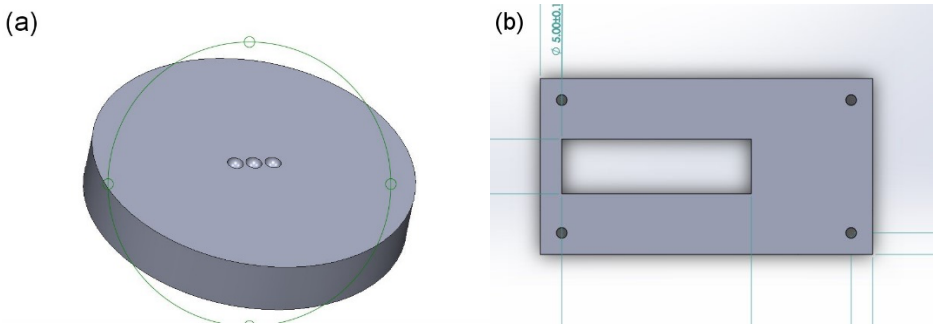

Figure S4. (a) The mold design for PC ball for fabricating the 3mm diameter plastic balls for tribology test and (b) The mold design for polymer-polymer interface adhesion test. Two identical dies were placed together in the opposite direction. Two flat plates (upper and bottom) held two dies with four pins on the corners to lock plates and dies in same place during the adhesion test.

Experimental details on fabrication of PC ball for tribology: Prior compression molding, a release agent (Stoner, silicon out mold release) was applied to the internal surface of the die. See die design in Figure S4. Sufficient polymer pellet was added to the die within different layer and a constant force (2200N), equivalent to ~1730 MPa, was applied for 5min. The molding temperature for the adhesion test was selected based on the minimum processing temperature for PC (240°C).

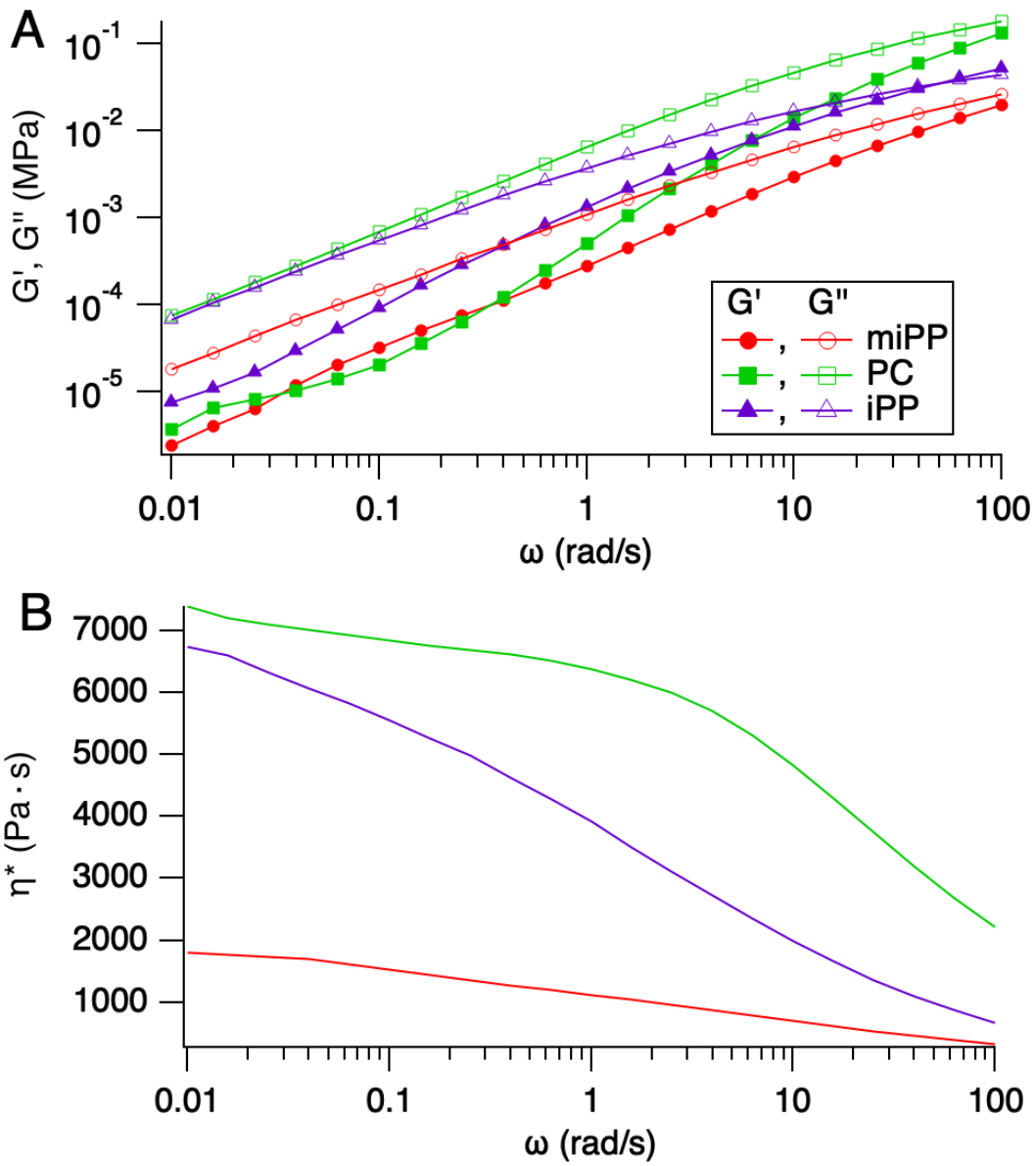

Figure S5. (A) Storage (closed symbols) and loss moduli (open symbols) and (B) complex viscosity for iPP, mPP, and PC from SAOS measurements at 240 °C and ε_0= 0.01.

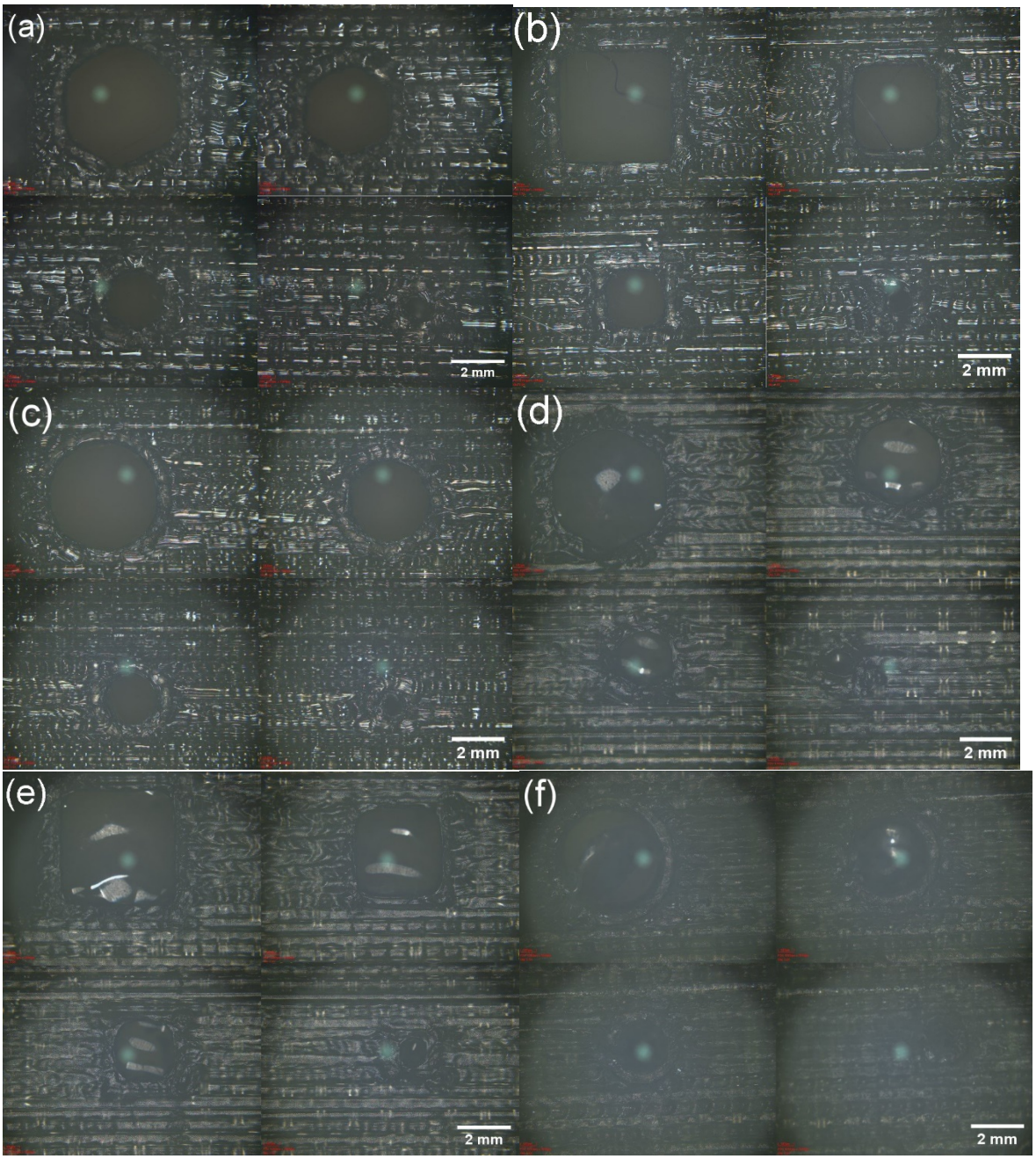
(a)
2 mm
(b)
2 mm
(c)
2 mm
(d)
2 mm
(e)
2 mm
(f)
2 mm

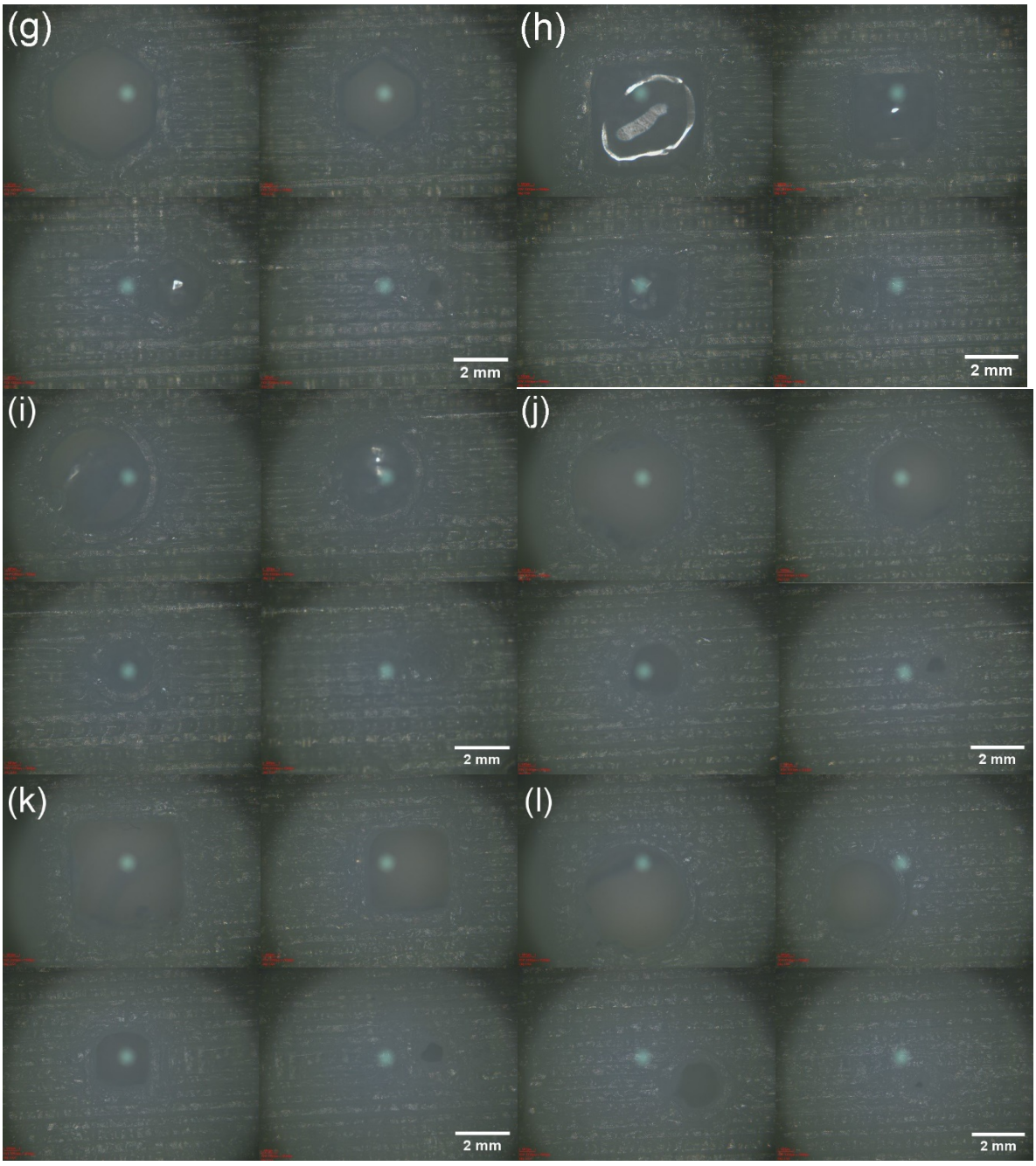

Figure S6. The individual holes on ASTM/ISO test specimen. The holes side are range from 4mm, 3mm, 2mm, and 1mm corresponding to top left, top right, bottom left and bottom right. (a) PC hexagon, (b) PC square, (c) PC circle, (d) iPP hexagon, (e) iPP square, (f) iPP circle, (g) iPP-PC hexagon, (h) iPP-PC square, (i) iPP-PC circle, (j) mPP-PC hexagon , (k) mPP-PC square, and (l) mPP-PC circle.

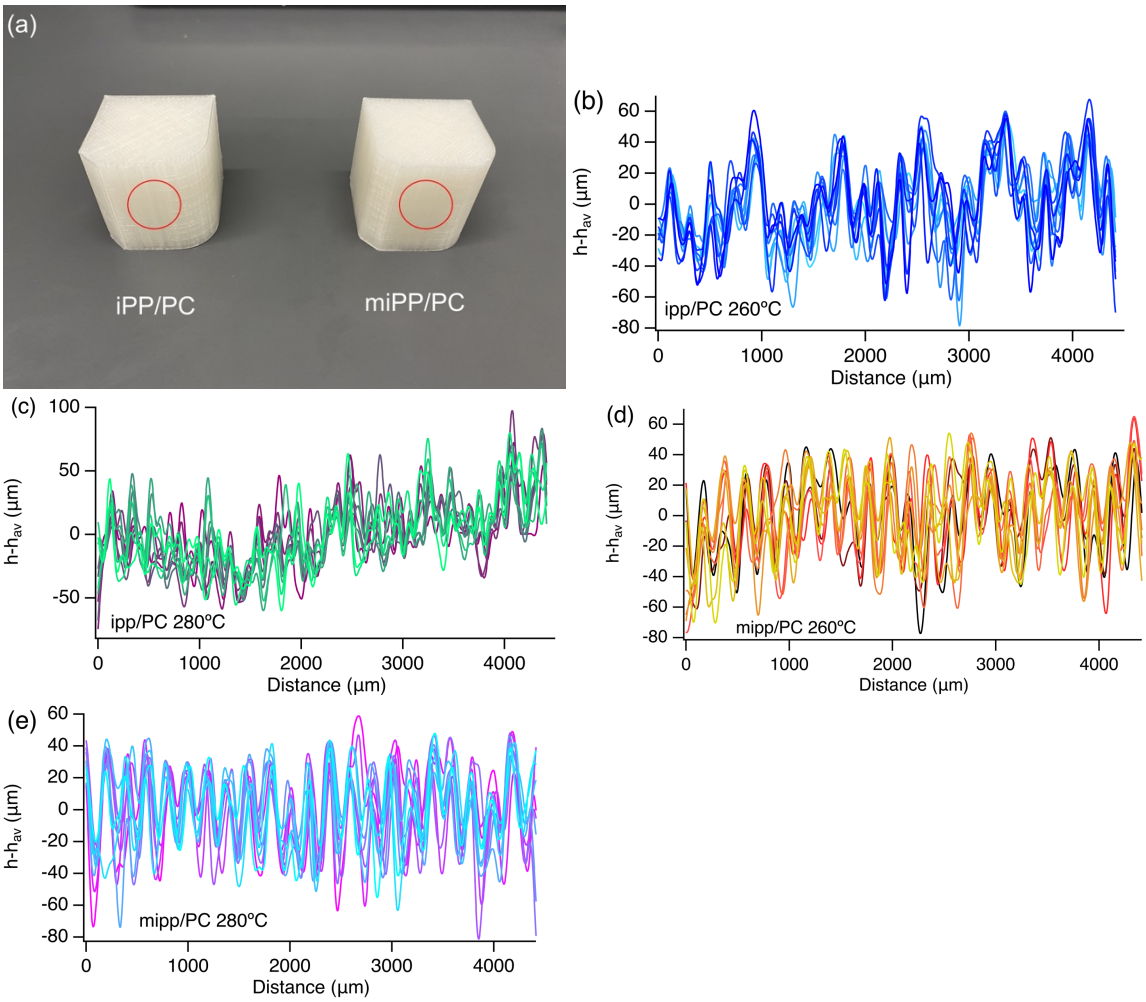

Figure S7. Surface topography of printed core-shell specimens is determined from (a) the side face (red circled area) of printed blocks. Multiple (10) line perpendicular to the printed road direction for iPP/PC at (b) 260 °C and (c) 280 °C and miPP/PC printed at (d) 260 °C and (e) 280 °C. The different colors correspond to cuts that are equally spaced across the profilometry profile (shown in Figure 3) at the print conditions noted.

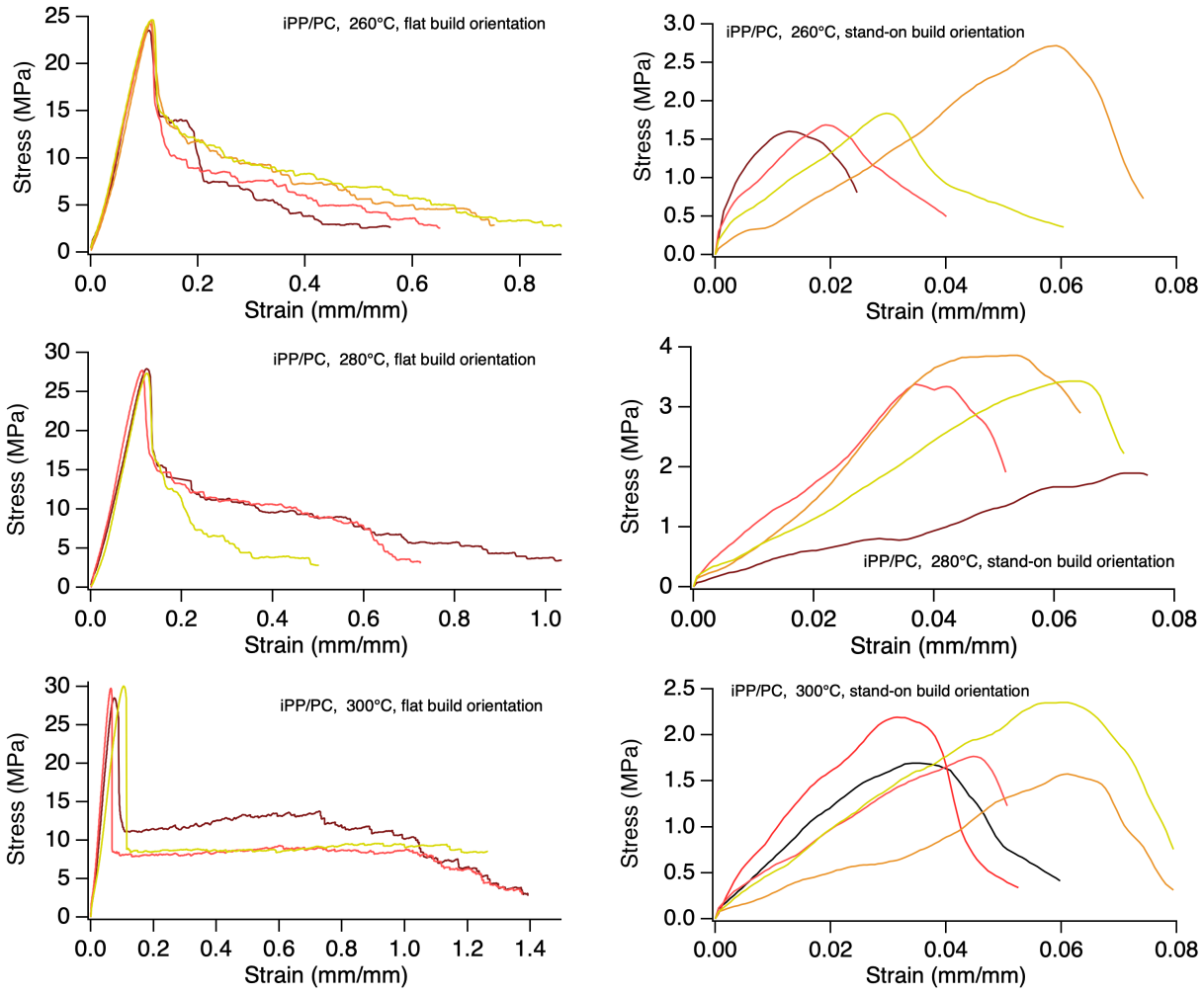

Figure S8. Stress-strain curves for 3D printed tensile bars using the iPP/PC filaments. The extrusion temperature and build orientation are provided on each panel. The strain is provided as calculated from the displacement of the grips in the UTS.

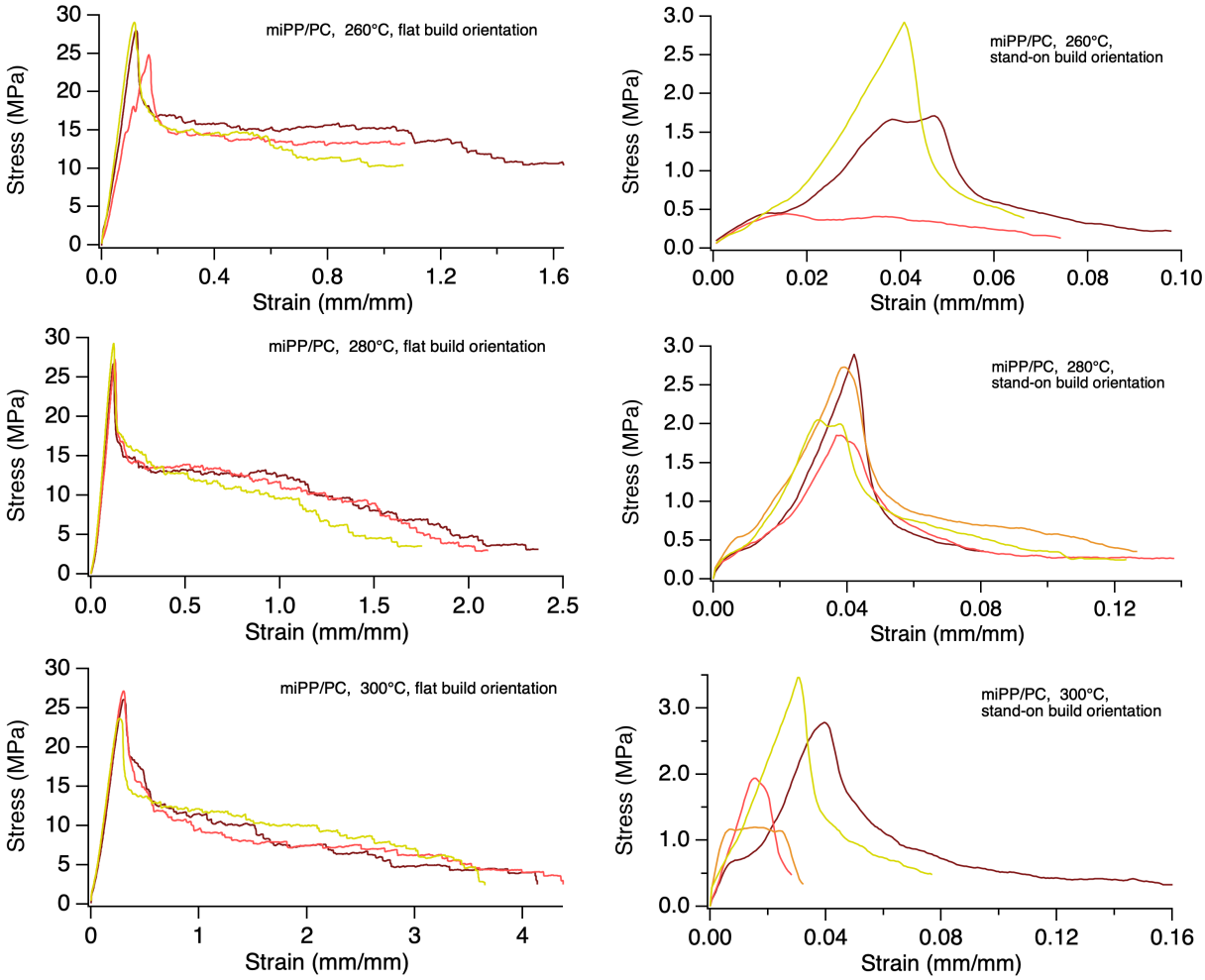

Figure S9. Stress-strain curves for 3D printed tensile bars using the miPP/PC filaments. The extrusion temperature and build orientation are provided on each panel. The strain is provided as calculated from the displacement of the grips in the UTS.

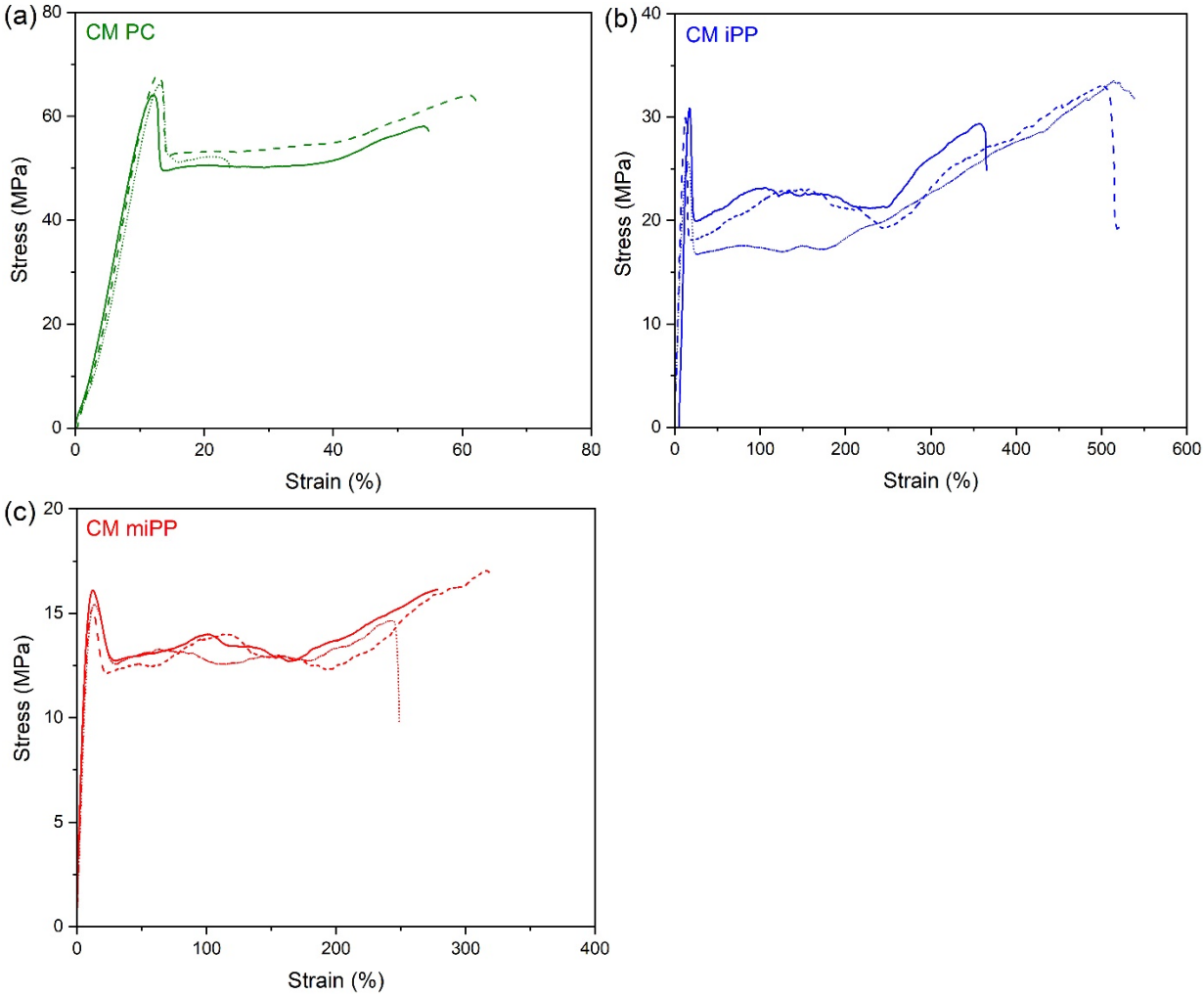

Figure S10. Stress-strain curves for the compression molded (a) PC, (b) iPP, and (c) mPP. The different lines correspond to different specimens of the same polymer.

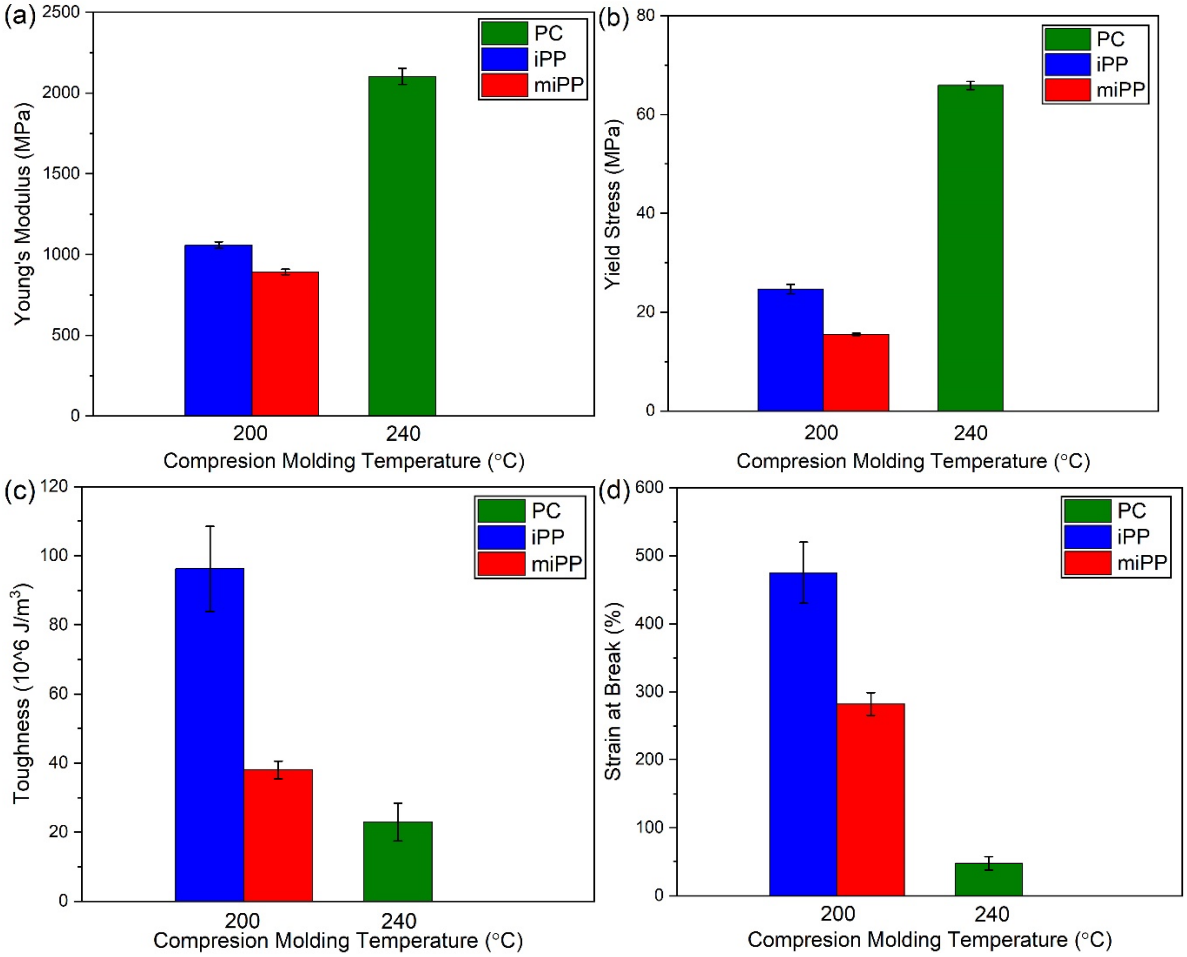

Figure S11. Summary of the tensile properties for the compression molded iPP, miPP and PC in terms of (a) Young's modulus, (b) yield stress, (c) toughness, and (d) strain at break.

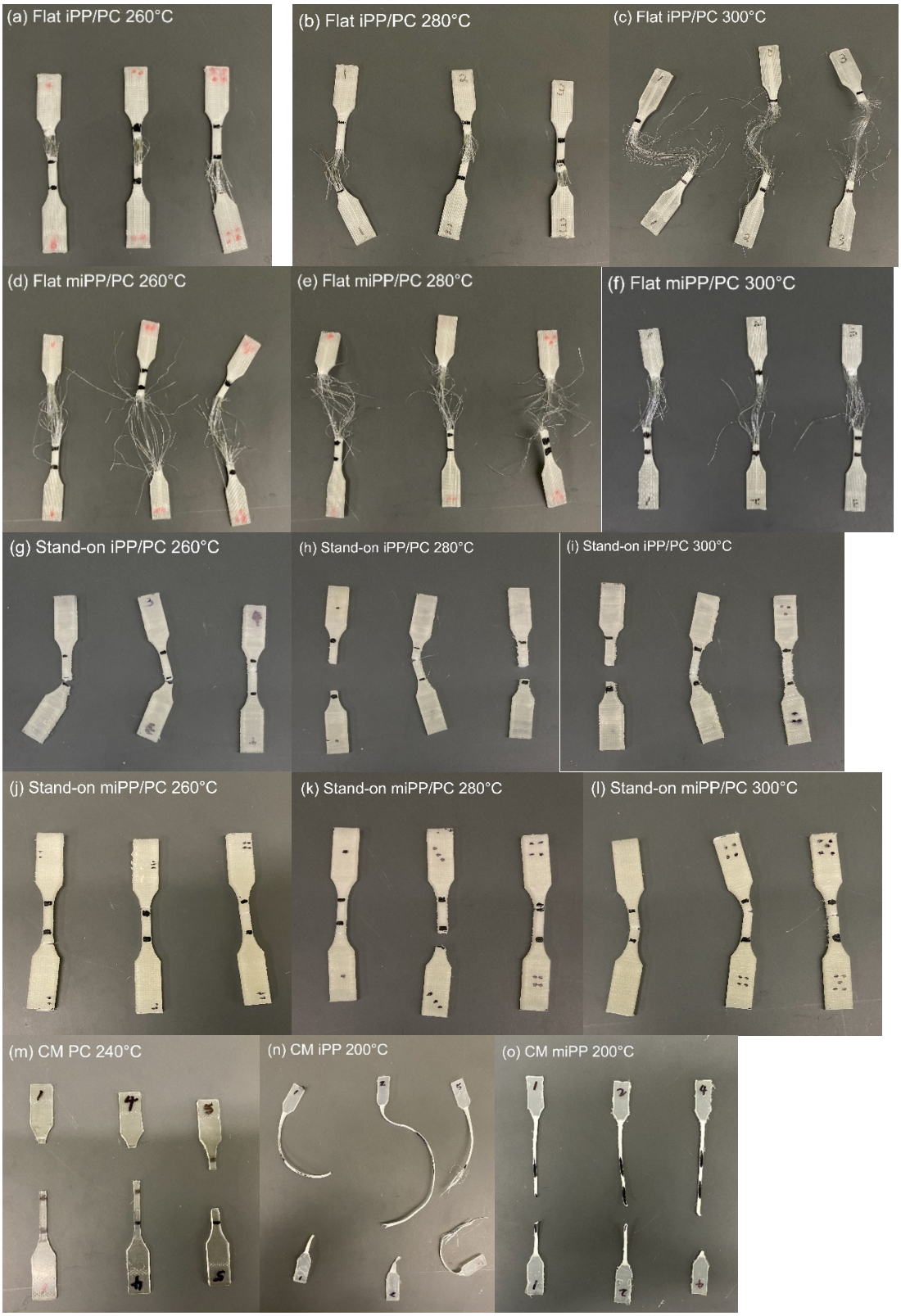

Figure S12. Images of the tensile bars post failure for 3D printed in flat orientation iPP (shell)-PC (core) at (a) 260 °C, (b) 280 °C and (c) 300 °C as well as mPP (shell) – PC (core) at (d) 260 °C, (e) 280 °C and (f) 300 °C. Images of the 3D printed tensile bars in stand-on orientation for iPP

(shell)-PC (core) at (g) 260 °C, (h) 280 °C and (i) 300 °C as well as mPP (shell) – PC (core) at (j) 260 °C, (k) 280 °C and (l) 300 °C. Images of the tensile bars post failure for compression molded (m) PC, (n) iPP and (o) mPP.

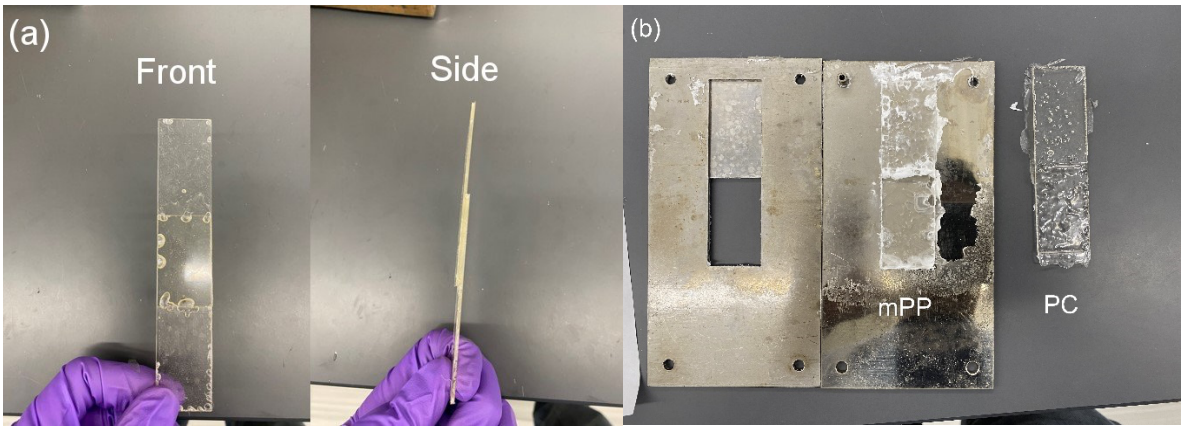

Figure S13. Photo of the lap shear test specimens before and after failure. (a) PC/PC lap shear joint and (b) miPP/PC lap shear joint. The miPP/PC lap shear joint would not be able to form enough adhesion due to the immiscibility in between PC and miPP. Similar failure of the iPP/PC lap shear joint occurred on demolding.

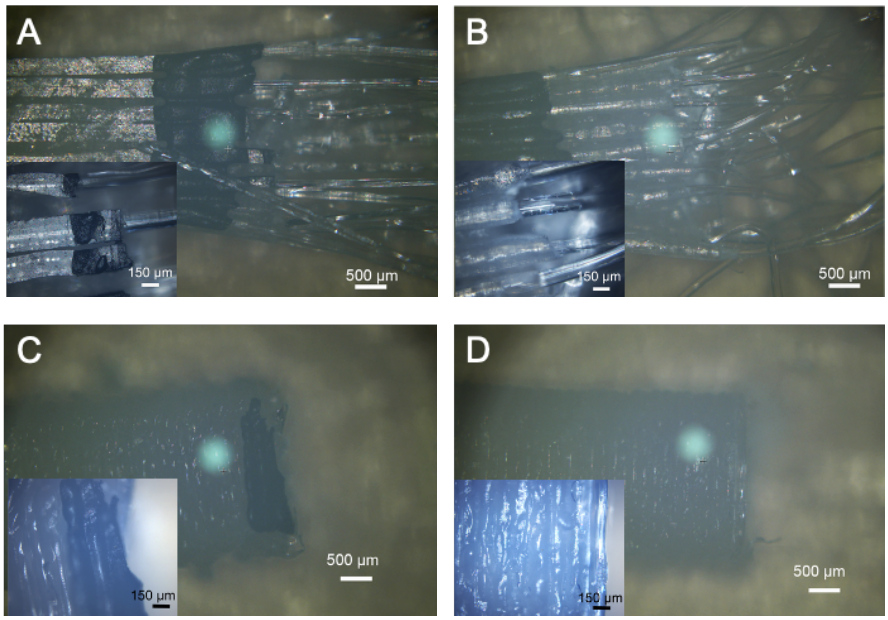

Figure S14. Optical images illustrating the top down view of the fracture surfaces for tensile specimens printed at 260 °C C for (A) iPP-PC in flat orientation, (B) mPP-PC in flat orientation, (C) iPP-PC in stand-on orientation and (D) mPP-PC in stand-on orientation. The insets illustrate a higher magnification view of the failure region.

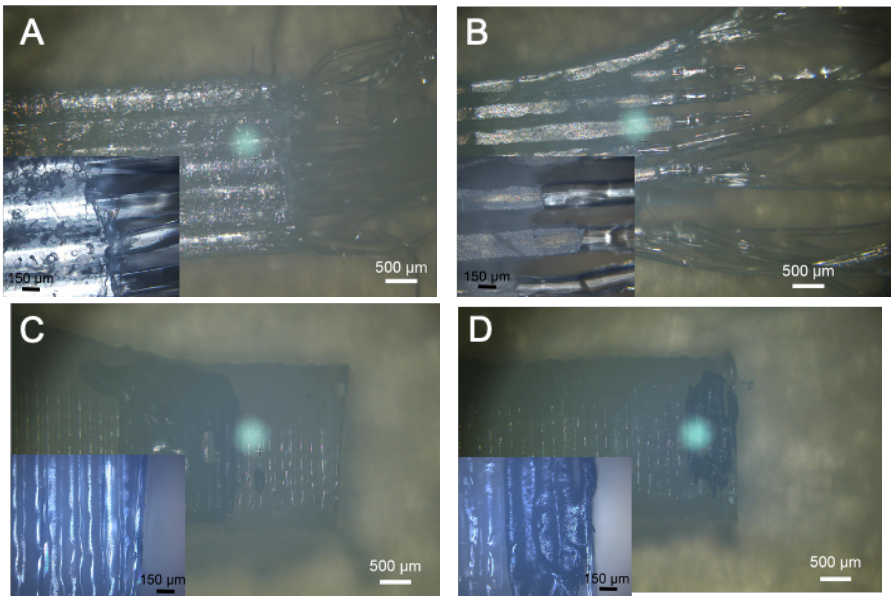

Figure S15. Optical images illustrating the top down view of the fracture surfaces for tensile specimens printed at 300 °C for (A) iPP-PC in flat orientation, (B) mPP-PC in flat orientation, (C) iPP-PC in stand-on orientation and (D) mPP-PC in stand-on orientation.

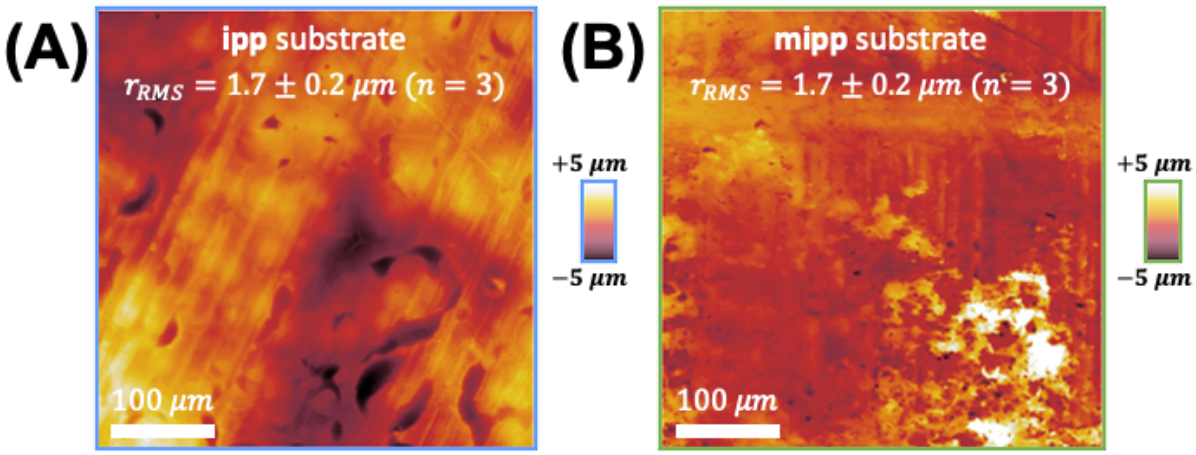

Figure S16. The average root mean square (RMS) surface roughness (r_{rms}) of the (A) ipp sheet and (B) mipp sheet used for the tribology measurements from optical profilometry utilizing a Zygo NewView 7300 instrument. The average was calculated from three measurements of each surface.